https://doi.org/10.5194/egusphere-2025-4454
Preprint. Discussion started: 29 September 2025

Simulating avalanche-triggered lake overspill and downstream impacts at Birendra Lake using RAMMS and HEC-RAS

Sujan Thapa[1], Ragini Vaidya[1], Mohan Bahadur Chand[1,2*], Rijan Bhakta Kayastha[1,2]

[1]Department of Environmental Science and Engineering, School of Science, Kathmandu University, Dhulikhel, Nepal

[2]Department of Environmental Science and Engineering, Himalayan Cryosphere, Climate and Disaster Research Centre (HiCCRDC), School of Science, Kathmandu University, Dhulikhel, Nepal

* Correspondence: mohan.chand@ku.edu.np

https://doi.org/10.5194/egusphere-2025-4454
Preprint. Discussion started: 29 September 2025

ABSTRACT

The study presents the first comprehensive quantitative assessment of avalanche-triggered GLOF hazards at Birendra Lake using integrated RAMMS-HEC-RAS modelling to evaluate cascading risks from avalanche release to downstream flood propagation. Three scenarios representing small (5.1×10^4 m³), medium (5.3×10^5 m³), and large (1.2×10^6 m³) avalanche releases from steep slopes (30°-48.8°) surrounding the lake were simulated. The modelling framework demonstrates that all scenarios reach Birendra Lake with substantial mass retention (62-86%), generating maximum velocities of 33.8-72.8 m/s and flow heights of 11.2-36.8 m. The displacement-driven overspill mechanism displaces 0.01-0.18% of total lake volume (4.7×10^6 m³), producing peak discharge rates of 615.7-3,151.8 m³/s. HEC-RAS flood modelling reveals rapid downstream propagation, with flood arrival times of 0.15-0.43 hours at Samagaon and 4.6-19.76 hours at Jagat, accompanied by maximum flood depths of 0.96-12.69 m and velocities of 1.94-15.62 m/s. The modelling results demonstrate strong qualitative alignment with the April 2024 event, validating the overspill mechanism. Medium to large avalanche scenarios pose severe threats to downstream communities, with the large scenario producing catastrophic conditions at Samagaun, where depths exceed 12 m with velocities above 15 m/s. The findings establish Birendra Lake as an imminent high-risk system where steep avalanche-prone terrain, lake proximity to unstable glacier zones, and significant downstream exposure create catastrophic cascading hazards. This research provides essential quantitative foundations for early warning systems and risk reduction strategies in avalanche-prone glacial lake environments across High Mountain Asia.

Keywords: Glacial Lake Outburst Flood, RAMMS, HEC-RAS, Birendra Lake, Climate Change

https://doi.org/10.5194/egusphere-2025-4454
Preprint. Discussion started: 29 September 2025

1. INTRODUCTION

1.1. Background

Global climate change is profoundly altering high-mountain environments, most notably through the accelerated retreat of glaciers and the associated formation and expansion of glacial lakes—trends especially pronounced in the Himalayas (Chand & Watanabe, 2018; Clague & Evans, 2000; Maskey et al., 2020). Recent research demonstrates ongoing climate warming and associated glacial lake expansion in the Himalayan region, with documented increases in lake area and corresponding glacier retreat over recent decades (Khadka et al., 2022). These lakes, frequently dammed by unstable moraine or ice barriers (Costa & Schuster, 1988), pose a growing risk of Glacial Lake Outburst Floods (GLOFs) to downstream communities and infrastructure (Worni et al., 2014). Several mechanisms can trigger GLOFs, among which mass movements—such as ice or snow avalanches impacting the lake surface—are particularly important (Emmer & Cochachin, 2013, Schneider et al., 2014). The impulse waves generated by such impacts have the potential to overtop or breach the impounding dam, leading to the sudden and catastrophic release of lake water (Heller et al., 2009).

A stark illustration of this cascading hazard occurred at Birendra Lake on 21 April 2024, when a massive ice-debris avalanche from the Manaslu Glacier triggered significant lake overtopping and downstream flooding (Maharjan et al., 2024). This event demonstrated the vulnerability of the lake system to avalanche impacts from the steep and heavily crevassed glacier snout, generating displacement waves that caused overspill and affected multiple settlements in the Budhi Gandaki valley (Maharjan et al., 2024). The terrain surrounding Birendra Lake exhibits high avalanche susceptibility, with steep slopes (>30°) dominating the upper basin and creating multiple potential release zones (Chaulagain et al., 2025). Understanding the hazard sequence from initial avalanche dynamics to potential lake overspill and downstream flooding in the Budhi Gandaki River valley is crucial for effective risk assessment and mitigation (Worni et al., 2015; Richards & Reddy, 2007).

Numerical modelling is essential in analysing and simulating these complex cascading processes (Worni et al., 2014). This investigation proposes the use of established tools, specifically RAMMS (Rapid Mass Movement Simulation):: Avalanche for simulating ice avalanche dynamics (Christen

https://doi.org/10.5194/egusphere-2025-4454
Preprint. Discussion started: 29 September 2025

et al., 2010; Casteller et al., 2008), alongside HEC-RAS (Hydrologic Engineering Center's River Analysis System) for modeling subsequent hydrological overspill and downstream flood propagation (Brunner, 2016; Feldman, 2000). The integration of these models enables a comprehensive simulation of the entire event chain, from avalanche impact to downstream effects (Worni et al., 2015), while also acknowledging inherent limitations—such as the adaptation of snow avalanche models for ice avalanches (Bartelt et al., 2012; Gauer et al., 2008) and challenges related to data scarcity, particularly limited lake bathymetric data (Huss et al., 2017; Østrem & Brugman, 1991).

1.2. Ice Avalanche Impact on Glacial Lakes

When an ice avalanche impacts the surface of a glacial lake, it transfers momentum to the water body, generating impulse waves (Zitti et al., 2016). The characteristics of these waves, including their amplitude and velocity, are influenced by several factors such as the volume and velocity of the impacting mass, the morphology of the lake basin, the Froude number, and the density difference between the avalanche material and the lake water (Zitti et al., 2016; Walder et al., 2003). Empirical models developed for landslide-generated waves are often adapted to simulate avalanche-induced waves; however, the lower density of snow and ice can lead to overestimations if these models are applied without modification (Zitti et al., 2016). Chisolm and McKinney (2018) conducted comprehensive three-dimensional (3D) lake-wave simulations for Lake Palcacocha in Peru, which provided critical insights into these dynamics. The volume released from the lake is consistently only a fraction (f) of the avalanche's initial ice volume. Specifically, their large-avalanche scenario resulted in 60% of the avalanche mass overtopping the dam, while medium and small scenarios yielded 50% and 30% overtopping, respectively. This established a representative displacement fraction (f) range of approximately 0.3–0.6 for such events. Furthermore, these avalanche-induced surges are inherently brief. Chisolm and McKinney (2018) reported that the initial wave overtopping for their large-avalanche case at Lake Palcacocha lasted approximately 100 seconds, with smaller avalanches producing overtopping durations of only 50-70 seconds. This finding is consistent with other studies indicating that GLOF wave generation by fast debris falls typically evolves within seconds to a few minutes. A direct consequence of these brief durations is that shorter pulse durations (T), typically 10–100 seconds (tens to hundreds of seconds), result in significantly higher peak flows for a given flood volume.

In the Himalayan context, avalanche-generated GLOFs exhibit comparable rapid behaviour,

https://doi.org/10.5194/egusphere-2025-4454
Preprint. Discussion started: 29 September 2025

reinforcing the applicability of these parameters. The 2016 Gongbatongsha event in the Poiqu/Bhotekoshi basin, triggered by a debris/rock avalanche into a small Tibetan Lake, demonstrated a modelled lake-emptying time of only a few minutes. Sattar et al. (2022) reconstructed this flood, with their best-fitting scenario indicating that the 0.12×10^6 m³ lake emptied in approximately 6 minutes, reaching a peak discharge of ~620 m³/s just 30 seconds after initiation. This suggests an exceptionally impulsive release. GLOF models for Imja Tsho in Nepal frequently employ impulse-wave inputs calibrated by rapid avalanche collapse, with the time from avalanche entry to terminal moraine run-up and subsequent outlet discharge estimated at approximately 3 minutes (Lala et al., 2018). Sattar et al. (2021) modelled avalanche impacts on Lower Barun Lake, reporting very short overtopping pulse durations of 20-21 seconds, accompanied by substantial peak discharges of 9,298 m³/s and 8,300 m³/s for two distinct avalanche scenarios, respectively.

The consistent reporting of short pulse durations (ranging from tens to hundreds of seconds, or a few minutes) and significant displacement fractions across diverse global (e.g., Palcacocha, Peru) and Himalayan (e.g., Gongbatongsha, Imja Tsho, Lower Barun) case studies provide a robust empirical and modelling precedent. This strong evidence base rigorously supports applying these parameters to Birendra Lake, underscoring that avalanche-triggered GLOFs are fundamentally impulsive events characterised by rapid water release and high peak flows. Accurately capturing this characteristic is critical for precise hazard assessment.

1.3. Integrated Avalanche and Hydraulic Modelling for Cascade Hazards

Integrating avalanche models like RAMMS with hydraulic models like HEC-RAS has been successfully applied in various case studies to simulate cascade hazards, particularly avalanche-triggered floods and landslides into lakes (Copernicus Emergency Management Service, 2025). For example, RAMMS has been used to simulate ice avalanches that subsequently triggered debris flows, highlighting the potential for cascading events (Mergili et al., 2022). In another study by Somos-Valenzuela et al. (2018), RAMMS was coupled with a hydrodynamic model (BASEMENT) to simulate avalanche-induced waves in a glacial lake. This then informed the simulation of moraine erosion and downstream flooding. These studies often use the outputs from the avalanche model, such as the volume and velocity of the mass at the point of impact with the lake, as input conditions for the hydraulic model to simulate the resulting flow or inundation.

https://doi.org/10.5194/egusphere-2025-4454
Preprint. Discussion started: 29 September 2025

HEC-RAS has been widely used to model the downstream flood propagation resulting from glacial lake outburst floods triggered by various mechanisms, including avalanches (Klimeš et al., 2014). These studies often involve reconstructing past GLOF events using field surveys and eyewitness accounts to calibrate the hydraulic models and assess the flood hazard in downstream areas. Integrated modelling approaches that link RAMMS simulations of avalanche impact with HEC-RAS simulations of lake overspill and downstream flooding provide a comprehensive framework for understanding the hazard chain (Somos-Valenzuela et al., 2018). These integrated models are crucial for identifying vulnerable areas, assessing the potential impacts on infrastructure and settlements, and developing effective mitigation measures for avalanche-triggered GLOF hazards (Copernicus Emergency Management Service, 2025).

1.4. GLOF and Avalanche Hazards in the Nepal Himalayas

The Nepal Himalayas is highly susceptible to glacial lake outburst floods (GLOFs) and avalanche hazards due to numerous glaciers and glacial lakes in a seismically active region undergoing rapid climate change (Carrivick & Tweed, 2016). Climate change is accelerating glacier retreat, leading to the formation and expansion of glacial lakes, thus increasing the risk of GLOFs (Byers et al, 2020, Carrivick & Tweed, 2016). Avalanches, including snow and ice avalanches, are significant triggers for GLOFs in this region, often causing displacement waves in glacial lakes that can overtop or breach moraine dams.

Birendra Lake, located at the base of the Manaslu Glacier in the Gorkha District of Nepal, experienced a notable flood event on April 21, 2024, which was triggered by a massive ice avalanche from the glacier snout (Mehar, 2024). This event caused a displacement wave in the lake, leading to overspill and flooding downstream, destroying a bridge (Fig. 1) is not a typical GLOF involving a moraine dam breach, highlights Birendra Lake's vulnerability to avalanche-triggered flooding (Maharjan et al., 2024).

Studies have indicated that even relatively small ice-snow avalanches can generate surge waves in Birendra Lake, leading to repeated GLOFs. The Manaslu region, in general, is prone to both glacial lake hazards and avalanches, necessitating further research to understand the potential for future cascading events (Mehar, 2024). Continuous monitoring of glacial lakes and glacier dynamics in the Manaslu region is crucial for effective risk assessment and the development of mitigation strategies. Here, in this paper we aimed estimating the potential cascading hazard posed by ice

https://doi.org/10.5194/egusphere-2025-4454
Preprint. Discussion started: 29 September 2025

avalanches originating from the Manaslu Glacier impacting Birendra Lake and triggering downstream flooding, using an integrated modelling approach with RAMMS::Avalanche and HEC-RAS, while explicitly acknowledging model and data limitations. We simulated the plausible ice avalanche scenarios using RAMMS::Avalanche with adjusted parameters to determine their runout characteristics and the volume of ice deposited into Birendra Lake. Similarly, we utilised HEC-RAS to model the hydrological response of Birendra Lake to the simulated ice avalanche inputs.

Figure 1 Bridge connecting Samagaun and Samdo (10 April 2025)

2. MATERIALS AND METHODS

2.1. Study Area

Birendra Lake is an end-moraine-dammed glacial lake in Chumanubri Rural Municipality, Gorkha District, Nepal (Fig. 2), occupying roughly 0.24 km² at about 3,632 m asl on the northeast base of Mount Manaslu (8,163 m). Remote-sensing and field observations confirm that the Manaslu Glacier has recently detached from direct contact with the lake, leaving a steep, heavily crevassed snout that is highly susceptible to ice-avalanche release and consequent water displacement (Maharjan et al., 2024). On 21 April 2024, such an avalanche generated an overspill flood with an estimated peak discharge of 32 m³/s (Maharjan et al., 2024) that destroyed the downstream footbridge at Samagaon, demonstrating the cascade hazard from slope instability to riverine impacts. The downstream areas of focus for this study along the Budhi Gandaki River include Samagaun (Site 1), Lhi (Site 2), Namrung (Site 3), Ghap (Site 4), Deng (Site 5), and Jagat (Site 6).

https://doi.org/10.5194/egusphere-2025-4454
Preprint. Discussion started: 29 September 2025

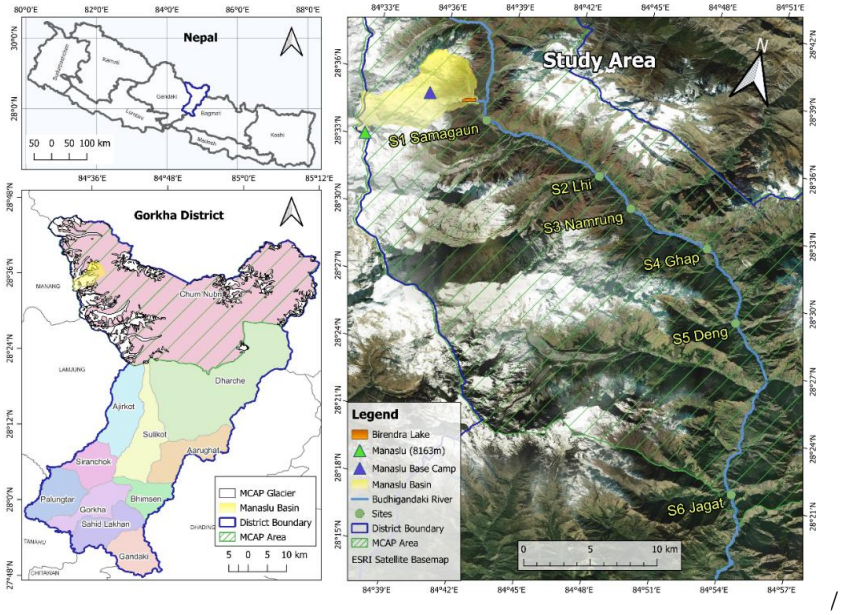

Figure 2 Study Area Map (© Google Maps 2025)

2.2. Data collection

A comprehensive dataset was assembled to support this study's integrated avalanche-flood modelling approach. A 12.5m resolution ALOS PALSAR DEM and a corrected 30 m resolution SRTM DEM were acquired to provide detailed topographic information of the study area, which is essential for accurately simulating surface processes and hydrological modelling. High-resolution optical satellite imagery from Planet Labs (Accessed April 2025) was utilised to estimate the lake's surface area, which is crucial for empirical lake volume calculations. Field observations, including geo-tagged photographs and qualitative insights from local interviews, were gathered during a site visit. The literature review provided the theoretical foundation and parameter calibration guidance for avalanche and flood modelling components. The flowchart of the study is provided in the Fig. 3.

2.2.1. Identification of Potential Avalanche Release Areas using GIS

Potential avalanche release zones were identified using the Bühler et al. (2013) multi-criteria methodology implemented in Google Earth Engine. This approach employs a rigorous binary classification system that categorises terrain as susceptible (value = 1) or non-susceptible (value = 0) to avalanche initiation. The methodology applies four simultaneous terrain criteria: slope angle

https://doi.org/10.5194/egusphere-2025-4454
Preprint. Discussion started: 29 September 2025

(28-60°), curvature (≤50), terrain roughness (≤15m standard deviation), and non-forested areas. Areas must satisfy all four criteria simultaneously to receive a classification of susceptible (1), while areas failing any single criterion are classified as non-susceptible (0). The Bühler methodology was originally validated against over 8,000 mapped avalanche release areas across the Swiss Alps and subsequently tested in the Indian Himalayas (Manali region, Himachal Pradesh), demonstrating strong transferability to high-mountain Asian environments. Selected susceptible zones were then filtered by minimum area (>780 m², approximately 5 pixels) to eliminate small, isolated areas unlikely to generate significant avalanches capable of reaching Birendra Lake, while ensuring adequate spatial extent for reliable RAMMS numerical simulation and proximity to Birendra Lake to identify three representative release scenarios for RAMMS simulation.

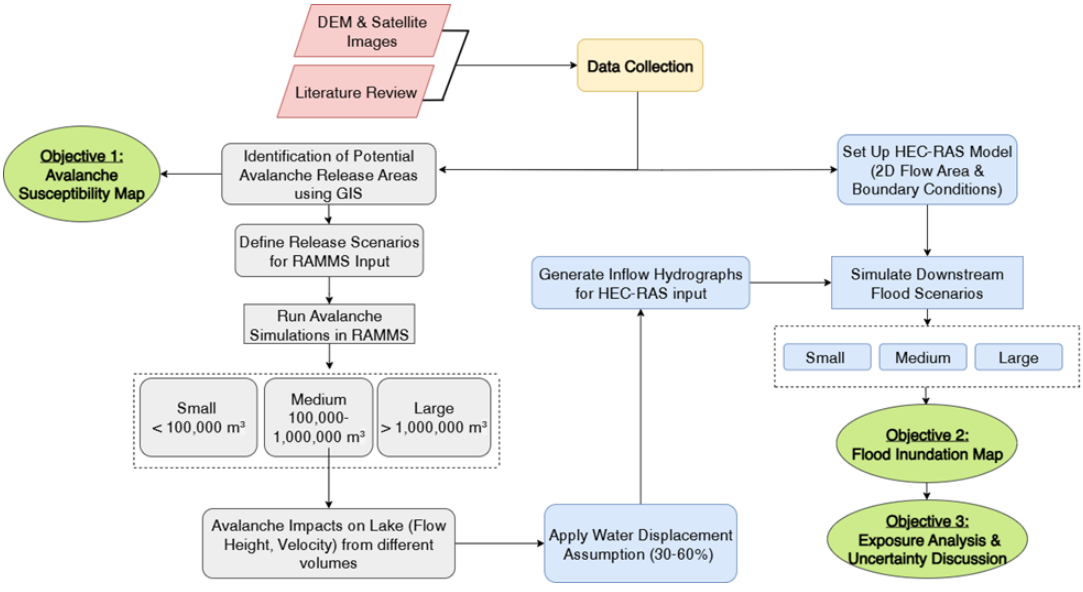

Figure 3 Flow Chart of Methodology

2.2.2. Define Release Scenarios for RAMMS Input

Ice avalanche scenarios were systematically developed based on identified potential release zones, and documented ice avalanche volume ranges from high-mountain environments. Recent comprehensive reviews of avalanche hazards in High Mountain Asia confirm the wide variability in avalanche magnitudes, with ice detachments from hanging glaciers and seracs capable of producing high-impact events (Acharya et al., 2023). Three distinct scenarios were defined with

https://doi.org/10.5194/egusphere-2025-4454
Preprint. Discussion started: 29 September 2025

varying release volumes: Small (≤100,000 m^3), Medium (100,000-1,000,000 m^3), and Large (>1,000,000 m^3). These volume ranges are consistent with documented ice avalanche magnitudes, where most break-off volumes in edge situations are well below 1 million m^3, while ramp situations can produce volumes exceeding 1 million m^3 (Alean, 1985). The classification accounts for the wide variability in ice avalanche volumes observed in recent events, ranging from 10^3-10^5 m^3 for smaller events to 10^5-10^6 m^3 for larger catastrophic events, as documented in recent assessments of cryospheric hazards in high mountain areas (Hock et al., 2019).

A consistent initial release depth of 5.0 meters was applied for all three scenarios, comparable to the 4.7m release depth used by Mandal et al. (2025) in the Lower Barun region and consistent with typical ice failure depths observed in similar Himalayan contexts. This standardised depth ensures that the substantial increase in volume from the Small to the Large scenario is primarily driven by expanding release area rather than varying initial thickness of ice failure, providing a systematic approach to scenario scaling that reflects natural avalanche formation processes.

2.2.3. Run Avalanche Simulations in RAMMS

A high-resolution digital elevation model (DEM) was imported into RAMMS::Avalanche to provide the topographic foundation for simulating avalanche flow paths. Release zones were systematically delineated for each scenario based on terrain steepness, glacier stability, and morphological characteristics. The material density was set to 1000 kg/m^3, representing consolidated ice conditions typical of glacial avalanches (Christen et al., 2010; Sattar et al., 2021). The Voellmy-Salm friction model was used to simulate avalanche dynamics, with a Coulomb friction coefficient (μ) of 0.12 and a turbulent friction coefficient (ξ) of 1000 m/s^2, consistent with parameter values commonly applied in ice avalanche modelling for Himalayan settings. These parameters were validated by Sattar et al. (2021) for the modelling of lake outburst and downstream hazard assessment at Lower Barun Glacial Lake and further applied by Mandal et al. (2025) in their Lower Barun region avalanche studies, supporting their applicability across similar high-mountain Himalayan environments.

2.2.4 Estimating Glacial Lake Volume

In many high-mountain regions worldwide, including the Himalayas, the lack of detailed bathymetric data for glacial lakes presents a significant challenge for hazard assessment and hydrological analysis (Huggel et al., 2002). Here, we also used equation proposed by Huggel et al.

https://doi.org/10.5194/egusphere-2025-4454
Preprint. Discussion started: 29 September 2025

(2002), which also adapted in in studies of glacial lakes in other mountainous regions, including the Himalayas, to estimate lake volumes where direct measurements are unavailable (Yao et al., 2012; Wang et al., 2018).

$$V = 0.104 \times A^{1.42}$$

Where V represents lake volume (m^3) and A denotes surface area (m^2).

2.2.5 Set Up HEC-RAS Model (2D Flow Area & Boundary Conditions)

Geometric data were prepared using DEM-extracted terrain data in HEC-RAS, representing Birendra Lake as a storage area and the downstream Budhigandaki River reach. The stage-storage relationship for the lake was defined based on DEM-derived area and estimated average depth using empirical area-volume relationships. Manning's roughness coefficient (n) was set to 0.06 for the main channel, representing typical conditions of Himalayan Mountain streams characterised by rocky beds, irregular banks, and moderate vegetation. This value falls within the established range of 0.030-0.070 for natural mountain channels (Chow, 1959). Given the limited field data available for precise roughness calibration, it provides a conservative estimate appropriate for flood hazard assessment.

2.2.6 Generate Flood Hydrographs from RAMMS Output

A point at the lake boundary with the highest flow height from RAMMS output was selected to create a time series of avalanche impact. This helped estimate the arrival time of the avalanche, the duration of lake disturbance, and the timing of peak flows. These values were used to develop a basic flood hydrograph without simulating detailed wave behaviour. Previous studies show that such overtopping events are very brief. For example, Chisolm and McKinney (2018) reported overtopping at Lake Palcacocha lasting about 100 seconds for a large avalanche, while smaller cases lasted 50 to 70 seconds. In the Himalayas, similar short pulse durations have been recorded. Sattar et al. (2022) found a 6-to-10-minute lake-emptying time at Gongbatongsha. Lower Barun Lake had pulse durations of 20 to 21 seconds with very high discharges (Sattar et al., 2021). These studies also suggest that only 30 to 60 per cent of the avalanche volume contributes to the actual flood discharge (Chisolm & McKinney, 2018). Although this method does not model impulse waves directly, it provides a simple and practical estimate of the lake response.

https://doi.org/10.5194/egusphere-2025-4454
Preprint. Discussion started: 29 September 2025

2.2.7 Simulate Downstream Flood Scenarios

HEC-RAS unsteady flow simulations were executed for each scenario (Small, Medium, Large) to simulate downstream flood propagation resulting from lake overspill. The modelling approach used converted RAMMS discharge hydrographs as inflow boundary conditions, with initial lake levels adjusted based on estimated water displacement volumes. The methodology assumes that avalanche-deposited ice displaces a volume of water of a different displacement fraction, leading to immediate overspill once the adjusted lake level exceeds the dam capacity. While not explicitly modelling impulse wave generation or complex avalanche-water interaction dynamics, this simplified approach provides conservative estimates of downstream flood impacts suitable for hazard assessment purposes (Westoby et al., 2014; Worni et al., 2014). The coupling methodology follows established mass flow to flood conversion practices in similar hazard assessment studies (Mergili et al., 2020).

2.2.8 Exposure Analysis and Uncertainty Discussion

Results across scenarios were analysed to understand sensitivity to avalanche volume and assess the cascade effect from ice avalanche to downstream flooding. Model outputs were compared with the peak-discharge estimates and inundation limits reported in Poudel (2025), providing a qualitative check that the simulated floods lie within the published range for Birendra Lake. The uncertainty discussion provides transparency regarding model limitations and guides the interpretation of results for further application.

3 RESULTS AND DISCUSSIONS

3.2 Glacial Lake Volume Calculation

Lake area determination from high-resolution satellite imagery yielded a delineated surface area of 0.246 km² (246,000 m²) for Birendra Lake (Table 1). Similarly, application of established empirical relationships developed by Huggel et al. (2002) produced a total lake volume of 4.7×10^6 m³ with an average depth of 19.11 m. These parameters represent critical baseline data for subsequent avalanche displacement modelling and risk assessment.

https://doi.org/10.5194/egusphere-2025-4454
Preprint. Discussion started: 29 September 2025

Table 1 Physical characteristics of Birendra Lake derived from Planet Labs satellite imagery analysis and empirical volume-area relationships

Parameter	Value	Units
Area	246000	m^2
Volume	4.7×10^6	m^3
Depth	19	m

The calculated volume provides essential baseline data for avalanche displacement modelling scenarios, which are presented in subsequent sections. The substantial depth-to-area ratio (19 m average depth across 0.246 km^2) indicates typical glacial lake morphology with significant water storage capacity characteristic of moraine-dammed systems. This 4.7×10^6 m^3 volume serves as the reference against which all displacement scenarios are evaluated, representing the total available water mass for potential overspill events.

The volume estimate's reliability is supported by consistency with regional glacial lake studies utilising similar empirical approaches, though the methodology inherently carries uncertainties associated with bathymetric assumptions. The 3 m spatial resolution of the Planet Labs imagery provides appropriate precision for lake area delineation at this scale. Future direct bathymetric validation would enhance precision for refined flood modelling applications, particularly for catastrophic scenario planning, where volume accuracy directly influences downstream hazard assessment and risk management strategies.

3.3 Avalanche Susceptibility Mapping

Avalanche susceptibility mapping for the Birendra Lake catchment area was conducted using the Bühler et al. (2013) multi-criteria methodology, which applies four simultaneous terrain parameters to produce binary classification (susceptible/not susceptible): slope angle (28-60°), curvature (≤50), terrain roughness (≤15m standard deviation), and non-forested conditions. This conservative approach ensures that only areas meeting all necessary physical conditions for avalanche formation are classified as susceptible, providing high confidence in release zone identification while eliminating false positives common in single-parameter assessments.

The susceptibility map (Fig 4) reveals strategically concentrated susceptible zones (red areas) around steep glacier margins and unstable ice formations adjacent to Birendra Lake, with the Manaslu climbing route traversing multiple identified susceptible areas. Comparison with

https://doi.org/10.5194/egusphere-2025-4454
Preprint. Discussion started: 29 September 2025

previous slope-based analysis by Chaulagain et al. (2025) demonstrates significant methodological advantages: while the slope-only approach classified extensive areas using three risk tiers (high: 30-45°, moderate: 10-30° & 45-60°, low: <10° & >60°), the Bühler multi-criteria method produces more spatially discrete and physically justified susceptible zones.

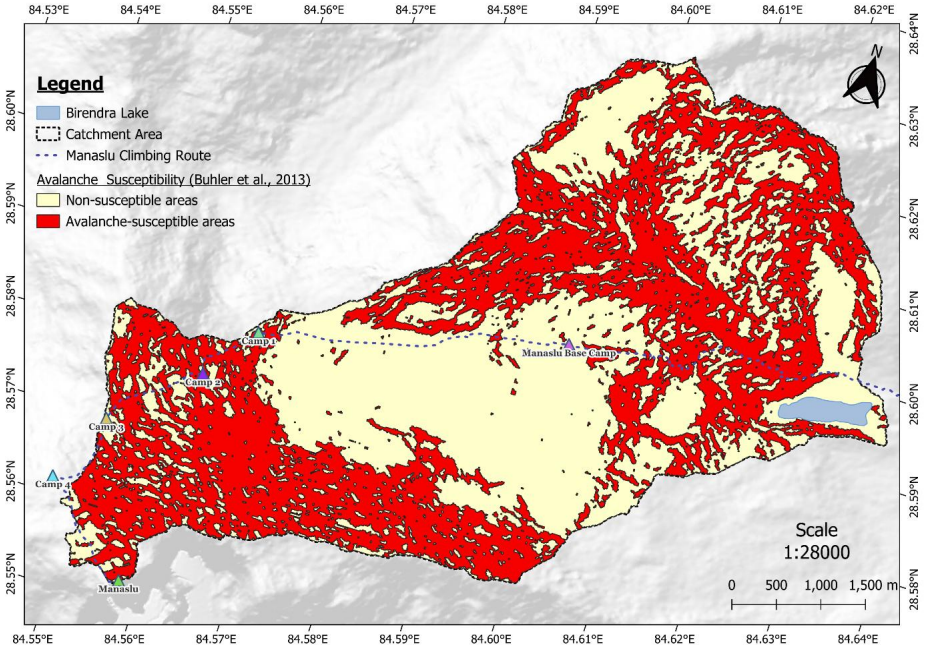

Figure 4 Avalanche susceptibility map of Birendra Lake catchment area based on Bühler et al. (2013) multi-criteria analysis, showing susceptible zones (red) and climbing route infrastructure.

The binary classification eliminates ambiguous "moderate risk" categories and focuses on terrain where all necessary physical conditions for avalanche formation exist simultaneously. This approach aligns with established practices in glacial hazard assessment, where terrain-based susceptibility mapping provides the foundation for process-based modelling applications. The methodology's robustness is particularly relevant for high-altitude environments where complex topographic interactions govern snow and ice stability.

This analysis systematically selected three representative release scenarios from identified susceptible polygons (>780 m² minimum area threshold), ensuring that subsequent RAMMS avalanche simulations originate from terrain with scientifically validated avalanche formation

https://doi.org/10.5194/egusphere-2025-4454
Preprint. Discussion started: 29 September 2025

potential rather than broad slope-based assumptions. The 780 m² minimum area threshold reflects DEM resolution constraints (12.5 m × 12.5 m pixels) and established best practices for meaningful avalanche release zone delineation in numerical modelling applications. The climbing route infrastructure and camp locations were adapted from Adventure Consultants' website (accessed June 2025), providing critical context for understanding exposure patterns along established mountaineering routes. This integration of hazard mapping with recreational infrastructure highlights the practical applications of susceptibility analysis for risk assessment and route planning in high-mountain environments.

3.4 Release Zone Selection and Scenario Development

A preliminary avalanche flow analysis was conducted across the entire Birendra Lake catchment using a standardised 1-meter release depth, with computational constraints limiting the basin-scale modelling resolution (Fig 5). The catchment-wide simulation revealed that avalanches originating from higher elevation zones lost momentum and deposited across extensive non-susceptible terrain in the central areas of the catchment (complete sequence in Appendix A), indicating minimal direct lake impact potential from distant release areas. This initial screening process demonstrated that topographic barriers and extended runout distances significantly attenuate avalanche energy before reaching the lake vicinity.

Based on these findings, subsequent analysis was refined to focus exclusively on release zones where avalanche flows demonstrated a clear trajectory toward Birendra Lake, ensuring realistic avalanche-lake interaction scenarios for downstream flood modelling. This targeted approach aligns with established best practices in glacial hazard assessment, where process-based modelling efficiency is optimised through strategic release zone selection rather than exhaustive basin coverage. The release area parameters for Birendra Lake show notable similarities and differences compared to other extensively studied Himalayan glacier lake systems. At Lower Barun Lake, the primary avalanche susceptibility was identified on south-facing slopes where ice-snow masses hang precariously on slopes between 45-60° (Sattar et al., 2021), comparable to Birendra's large scenario mean slope of 48.8°. Field observations at Lower Barun documented avalanche volumes of approximately 1.12×10^5 m³ of ice-snow, with modelled events reaching 9.2×10^5 m³ (Sattar et al., 2021), which falls within the range of Birendra's medium to large scenarios.

https://doi.org/10.5194/egusphere-2025-4454
Preprint. Discussion started: 29 September 2025

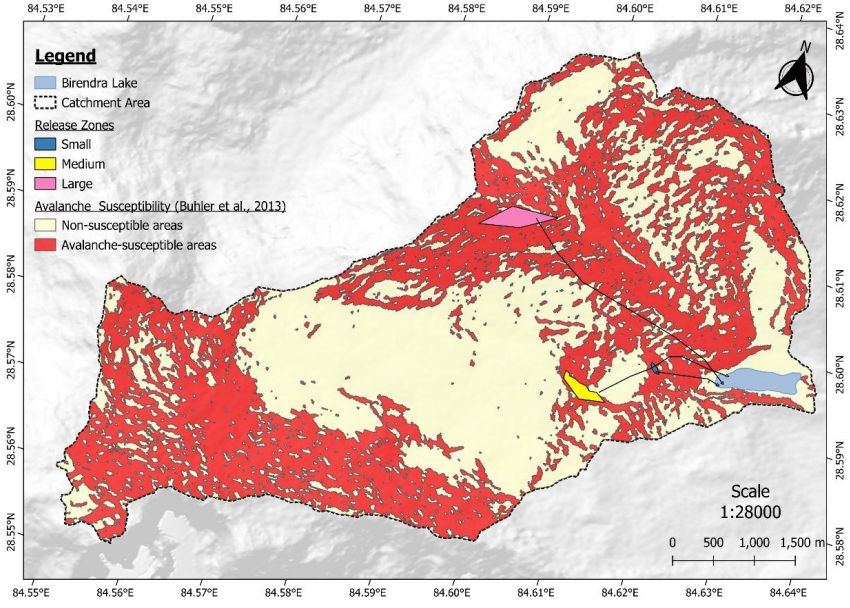

Figure 5 Potential release zones identification for RAMMS input showing three scenario classifications: small (blue), medium (yellow), and large (pink) based on Bühler et al. (2013) susceptibility mapping and preliminary flow trajectory analysis

Table 2 RAMMS release area properties for three avalanche scenarios derived from susceptibility mapping and trajectory analysis

Parameter	**Value**		
	Small	**Medium**	**Large**
Mean slope angle **(**°)	43.3	44.8	48.8
Mean altitude **(**m)	4,130	4,510	5,770
Projected area **(**m²)	7,300	73,300	145,000
Initial Release volume **(**m³)	51,200	534,000	1,165,000

Note: Values reflect appropriate precision based on 12.5 m×12.5 m DEM resolution (±156 m² pixel uncertainty) and established uncertainty propagation principles in glacial hazard modeling.

At Palcacocha Lake in Peru, avalanche scenarios modelled volumes ranging from 0.15×10^6 m³ (small) to 1.8×10^6 m³ (large) (Chisolm & McKinney, 2018), with the large scenario volume being significantly higher than Birendra's largest modelled event. The Palcacocha study identified release

https://doi.org/10.5194/egusphere-2025-4454
Preprint. Discussion started: 29 September 2025

zones with slopes between 45-60° and applied similar density assumptions of 1000 kg/m³ for ice-dominated avalanches (Schneider et al., 2014), consistent with the parameters used in the Birendra analysis. Three distinct ice avalanche scenarios (small, medium, and large) were defined based on release zones identified through the Bühler et al. (2013) multi-criteria susceptibility analysis to investigate a range of potential events. The parameters for these scenarios, detailed in Table 2, were selected to represent systematic progression in event magnitude with physically meaningful scaling relationships based on observed patterns from comparable Himalayan systems. The Small scenario simulates a localised release of 51,200 m³ from a 7,300 m² area at a mean altitude of 4,130 m, representing typical slope instability events common in glaciated high-mountain environments.

The Medium scenario scales significantly, with a release volume of 534,000 m³, representing a nearly tenfold increase in avalanche magnitude. This scenario originates from a higher elevation (4,510 m) and steeper terrain (44.8°), reflecting upper glacier zones' enhanced gravitational potential and slope instability. The Large scenario models a catastrophic event from the highest and steepest parts of the catchment area, with a release volume of 1,165,000 m³ from a 145,000 m² area at a mean elevation of 5,770 m and slope angle of 48.8°. For all three scenarios, a consistent initial release depth of 5.0 meters was applied, comparable to the 4.7-4.9 m depths used by Mandal et al. (2025) and Sattar et al. (2021) in the Lower Barun region and typical ice failure depths in similar Himalayan contexts. This standardisation ensures that volume increases from Small to Large scenarios are driven by expanding release area rather than variable failure thickness, providing physically consistent scaling relationships. The reported precision acknowledges inherent DEM-derived uncertainties while maintaining sufficient accuracy for hazard assessment and downstream flood modelling.

3.5 RAMMS Simulation Results

RAMMS avalanche simulations were conducted for the three defined scenarios to quantify flow dynamics, impact parameters, and lake deposition characteristics. The numerical modelling reveals fundamental relationships between release volume, flow behaviour, and downstream impact potential that are critical for understanding avalanche-lake interaction dynamics at Birendra Lake.

3.5.4 Flow Dynamics and Impact Parameters

The avalanche simulations demonstrate clear escalation patterns across the three scenarios, with

https://doi.org/10.5194/egusphere-2025-4454
Preprint. Discussion started: 29 September 2025

dynamic parameters showing systematic increases reflecting larger events' enhanced destructive potential. Maximum flow velocities exhibit substantial scaling, ranging from 33.8 m/s for the small scenario to 72.8 m/s for the large scenario, indicating the potential for extremely high-speed ice flows in major avalanche events. These velocities exceed typical threshold values for catastrophic impact and are consistent with observations from similar Himalayan avalanche events. Maximum flow heights increase dramatically across scenarios, from 11.2 m (Small) to 36.8 m (Large), demonstrating the substantial vertical extent of ice avalanche flows. The maximum impact pressures show the most dramatic scaling relationship, ranging from 1,145 kPa in the small scenario to 5,295 kPa in the large scenario. These impact forces can cause severe structural damage and generate significant water displacement upon lake impact, highlighting the destructive potential of larger avalanche events.

The computational error between initial and RAMMS-calculated release volumes remained below 5% across all scenarios, demonstrating acceptable model precision for hazard assessment applications. This level of accuracy is consistent with established RAMMS modelling standards and provides confidence in the reliability of the flow dynamics and impact parameters derived from the simulations.

Table 3 RAMMS simulation summary showing dynamic parameters and lake deposition characteristics for three avalanche scenarios

Parameters	**Value**		
	Small	**Medium**	**Large**
RAMMS computed release volume (m^3):	53,100	528,000	1,171,000
Volume reaching lake (m^3):	45,900	328,000	845,000
Release volume reaching lake (%):	86.5	62.1	72.2
Overall max velocity (m/s):	33.8	48.1	72.8
Overall max flow height (m):	11.2	28.2	36.8
Overall max pressure (kPa):	1,150	2,320	5,300

https://doi.org/10.5194/egusphere-2025-4454
Preprint. Discussion started: 29 September 2025

3.5.5 Lake Deposition Efficiency

The lake deposition volumes reveal that substantial portions of the released ice material reach Birendra Lake, with absolute volumes ranging from 45,900 m³ (small) to 845,000 m³ (large). However, the percentage of release volume deposited shows non-linear behaviour that provides important insights into avalanche transport mechanics. The small scenario achieves the highest deposition efficiency at 86.5%, the medium scenario shows the lowest at 62.1%, and the large scenario reaches 72.2%. This variation suggests that larger avalanches experience greater material loss during transport due to entrainment processes, deposition along the flow path, or lateral spreading effects. Conversely, smaller avalanches may follow more direct paths to the lake with higher material retention efficiency, possibly due to better topographic confinement and reduced opportunity for material dispersal during transport.

3.5.6 Spatial Flow Patterns and Lake Impact Potential

The simulation results reveal distinct spatial patterns that reflect the influence of release volume and topographic constraints on flow behaviour. Figures 6, 7, and 8 illustrate the RAMMS avalanche simulation results, showing distinct differences in flow extent, height distribution, and lateral spreading characteristics across the three scenarios. The estimated release volumes in the figures refer to the initial release volumes, and computational error between initial and RAMMS-calculated release volumes remained below 5% across all scenarios, demonstrating acceptable model precision for hazard assessment applications.

The Small scenario (Fig 6), with a release volume of 53,100 m³, follows the most direct path to Birendra Lake. It remains highly channelised by the natural topography, resulting in a narrow flow corridor that efficiently reaches the lake with minimal lateral spreading (see supplementary Appendix B). This behaviour maximises transport efficiency and explains the higher deposition percentage observed for this scenario. The Medium scenario (Fig 7), originating from a 528,000 m³ release, presents a more constrained but still powerful flow. It remains within the main valley system but exhibits significant lateral spreading and material loss along its path before terminating in the lake. This scenario represents a transitional behaviour between fully confined and unconfined flow regimes (see supplementary Appendix C). The Large scenario (Fig 8), with a release volume of 1,171,000 m³, generates the most extensive flow pattern. Its immense volume and high starting elevation cause the flow to impact Birendra Lake and spill over an eastern ridge, creating a broad

https://doi.org/10.5194/egusphere-2025-4454
Preprint. Discussion started: 29 September 2025

path with lateral spreading exceeding 1 km (see supplementary Appendix D). This multi-directional flow behaviour demonstrates how catastrophic events can exceed natural topographic confinement, potentially affecting areas beyond the primary drainage basin.

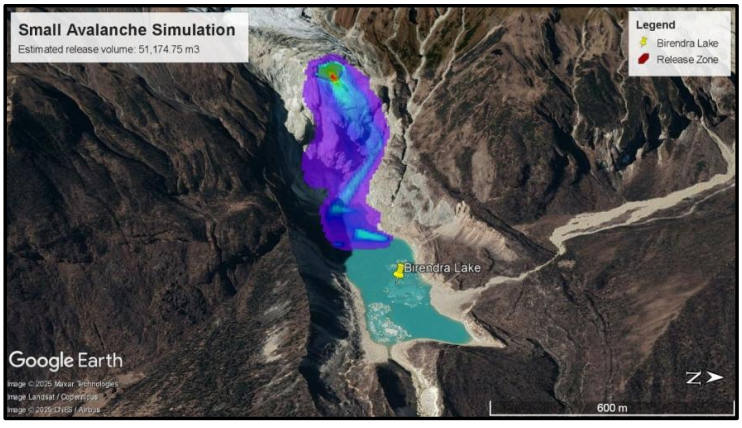

Figure 6 Small avalanche simulation flow extent illustrating highly channelised flow following natural topographic corridors (© Google Maps 2025)

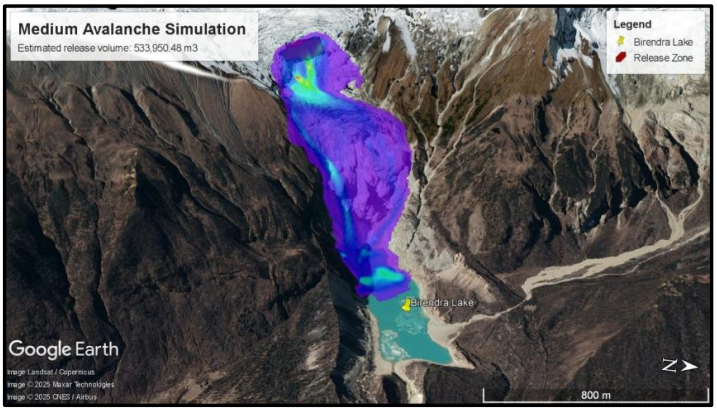

Figure 7 Medium avalanche simulation flow extent demonstrating valley-confined flow with moderate lateral expansion (© Google Maps 2025)

Across all scenarios, the colour gradient (purple to yellow, indicating increasing flow height) highlights flow concentration patterns and demonstrates how topographic controls influence avalanche behaviour. Despite their different spatial patterns, all three scenarios demonstrate direct impact potential on Birendra Lake, confirming that these source areas represent viable triggers for cascading displacement floods and validating the susceptibility mapping approach used for release

https://doi.org/10.5194/egusphere-2025-4454
Preprint. Discussion started: 29 September 2025

zone identification.

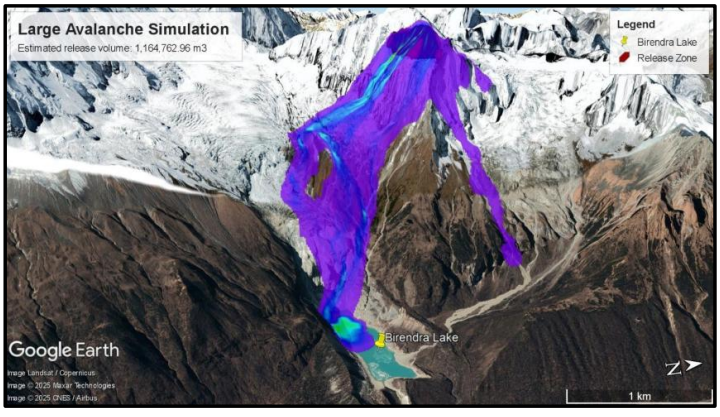

Figure 8 Large avalanche simulation flow extent showing maximum lateral spreading and multi-directional flow patterns (© Google Maps 2025)

3.6 HEC-RAS Inflow Hydrographs for Various Avalanche Scenarios

The outputs from the RAMMS simulations were translated into inflow hydrographs for the HEC-RAS model, representing the initial flood pulse generated by avalanche impact and subsequent water displacement. Following the methodology established by Chisolm and McKinney (2018) for avalanche-induced lake displacement events, three displacement fractions (30%, 45%, and 60%) of the deposited avalanche volume were applied to represent a range of plausible lake responses, accounting for inherent uncertainties in impulse wave dynamics and lake-avalanche interaction mechanisms. This approach acknowledges that displacement efficiency varies based on impact velocity, avalanche density, and lake bathymetry, with the 45% displacement scenario serving as the primary basis for downstream flood analysis. The resulting hydrographs for the small, medium, and large scenarios are presented in Figures 9, 10 and 11.

https://doi.org/10.5194/egusphere-2025-4454
Preprint. Discussion started: 29 September 2025

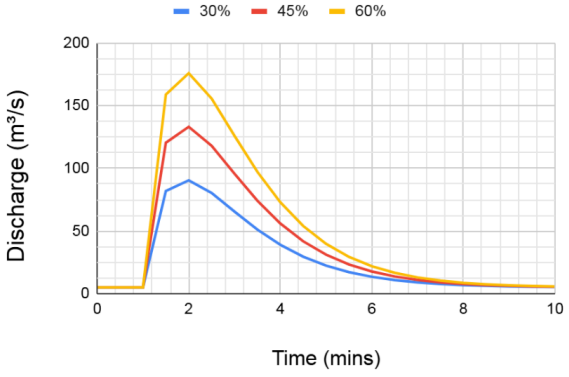

Figure 9 Small avalanche scenario flood hydrograph showing characteristic impulsive discharge pattern with peak flows ranging from 90.4-175.9 m³/s across three displacement scenarios (blue = 30%, red = 45%, orange = 60% displacement fractions)

Small Scenario (Fig 9): For the smallest avalanche (51,200 m³ estimated release volume), the resulting flood hydrograph shows peak discharges ranging from 90.4 m³/s for a 30% displacement to 175.9 m³/s for a 60% displacement. The 45% displacement scenario generates a peak flow of 133.2 m³/s, representing a significant but localised flood event. While modest compared to larger scenarios, these flows exceed typical seasonal discharge variations and are sufficient to initiate downstream flooding with potential impacts on valley-floor infrastructure.

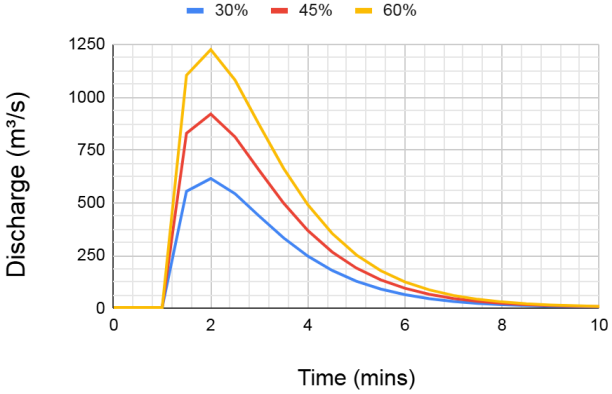

Figure 10 Medium avalanche scenario flood hydrograph demonstrating substantial discharge amplification with peak flows ranging from 615.7-1,226.4 m³/s across displacement scenarios (blue = 30%, red = 45%, orange = 60% displacement fractions).

Medium Scenario (Fig 10): The medium avalanche scenario (534,000 m³ estimated release volume) produces a drastically larger flood pulse with peak discharges increasing substantially, ranging

https://doi.org/10.5194/egusphere-2025-4454
Preprint. Discussion started: 29 September 2025

from 615.7 m³/s (30% displacement) to a formidable 1,226.4 m³/s (60% displacement). The 45% scenario peak of 921.0 m³/s marks a critical threshold where flood magnitude transitions from localised impact to potentially catastrophic downstream effects. This scaling demonstrates the non-linear relationship between avalanche volume and resultant flood severity, consistent with observations from similar Himalayan GLOF events.

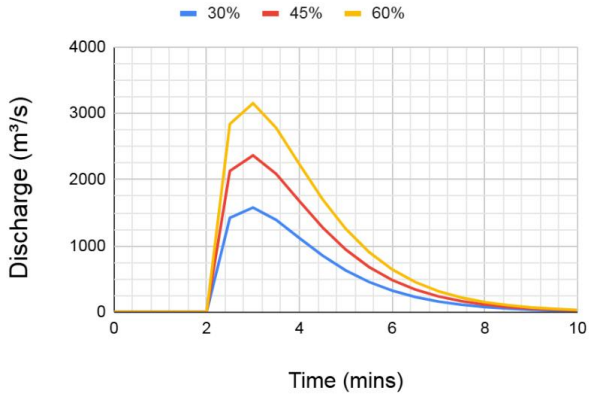

Figure 11 Large avalanche scenario flood hydrograph showing catastrophic discharge potential with peak flows ranging from 1,578.4 - 3,151.8 m³/s across displacement scenarios (blue = 30%, red = 45%, orange = 60% displacement fractions)

Large Scenario (Fig 11): Representing a catastrophic failure from the upper glacier zones, the large scenario (1,165,000 m³ estimated release volume) generates exceptionally high peak flows. The discharge ranges from 1,578.4 m³/s (30% displacement) to a massive 3,151.8 m³/s (60% displacement), with the 45% scenario peaking at 2,365.1 m³/s. Such discharge magnitudes are comparable to major GLOF events documented in the Himalayan region and would be capable of causing widespread and severe destruction to downstream communities and infrastructure.

Temporal Characteristics and Warning Implications

The hydrographs for all scenarios share a characteristic morphology: a rapid, single-peaked pulse with a steep rising limb and a slightly less steep falling limb. This pattern is consistent with impulsive, short-duration events where flood energy is released over minutes rather than hours, aligning with documented avalanche-triggered GLOF behaviour from comparable Himalayan systems (Sattar et al., 2022; Maharjan et al., 2024). The entire significant outflow for all scenarios occurs within approximately 8-10 minutes, which is consistent with the 6-minute lake-emptying time observed in the 2016 Gongbatongsha event (Sattar et al., 2022) and the 3-minute avalanche-

https://doi.org/10.5194/egusphere-2025-4454
Preprint. Discussion started: 29 September 2025

to-discharge timeframe documented at Imja Tsho (Lala et al., 2018). This temporal compression underscores the limited time for downstream warning and emergency response. This rapid onset is particularly critical for hazard management in the Manaslu region, as it eliminates traditional flood warning lead times observed in conventional riverine flooding scenarios and necessitates pre-positioned emergency response capabilities rather than reactive measures. The brief duration also amplifies peak discharge rates, as the same displaced volume concentrated into shorter periods generates significantly higher instantaneous flows, a phenomenon well-documented in avalanche-triggered GLOF events across the Himalayas (Worni et al., 2014; Wang et al., 2018)

Sensitivity Analysis and Hazard Assessment Implications

The analysis of these inflow hydrographs demonstrates that the resultant flood magnitude is highly sensitive to the initial avalanche volume and the assumed ice-water displacement efficiency. The non-linear increase in peak discharge from Small (133.2 m^3/s) to Large (2,365.1 m^3/s) scenarios—representing an 18-fold amplification despite only a 23-fold increase in avalanche volume—highlights the critical importance of accurately identifying potential release volumes for hazard assessment in glaciated mountain environments (Christen et al., 2010; Gabl et al., 2017). The displacement fraction sensitivity is equally significant, with 60% displacement scenarios generating 1.8-2.0 times higher peak flows than 30% scenarios across all avalanche magnitudes. This sensitivity underscores the importance of continued research into avalanche-lake interaction dynamics. It validates the conservative 45% displacement assumption adopted for primary hazard modelling applications in this study, aligning with established Himalayan GLOF modelling practices.

3.7 Exposure analysis of Avalanche-induced flood scenarios at different sites

The scenario-based exposure analysis of avalanche-induced Glacier Lake Outburst Floods (GLOFs) at six different downstream sites offers critical insights into how the magnitude of such events impacts the spatial extent of inundation, flood depth, and exposure to infrastructure. This comparative study of Scenario 1 (small), Scenario 2 (medium), and Scenario 3 (large) highlights significant differences in hazard levels across varied terrain settings and settlement patterns. By assessing inundation patterns and interpreting flood behaviour at each site, this analysis contributes to understanding both immediate and extended risks posed by GLOFs in vulnerable Himalayan regions.

https://doi.org/10.5194/egusphere-2025-4454
Preprint. Discussion started: 29 September 2025

575 **Table 4** Lake Displacement Analysis

	Small	Med	Large
Total Avalanche Volume Outflow (m^3)	45,900	328,100	845,300
Total Lake Volume Overspill (%)	0.01	0.07	0.18

Table 4 demonstrates the direct relationship between avalanche magnitude and lake displacement volumes under the 45% displacement assumption. The Small scenario generates minimal outflow (45,900 m³, 0.01% of lake volume), while the Medium and Large scenarios produce substantially greater displacements of 328,100 m³ (0.07%) and 845,300 m³ (0.18%) respectively. Despite substantial volume increases, all scenarios displace less than 0.2% of total lake capacity, indicating overspill rather than complete drainage as the primary flood mechanism. This finding suggests that Birendra Lake would remain largely intact even under catastrophic avalanche impacts, with displaced water volumes serving as the primary driver of downstream flooding rather than complete lake breach scenarios.

The results of the HEC-RAS flood modelling are presented in Table 5. Moreover, as visualised in Figure 12, a clear progression of hazard severity corresponds to the magnitude of the initial avalanche. In Scenario 1 (Small), the flood is a low-impact but far-reaching event. It arrives at Site 1 (Samagaon) in 0.43 hours with a shallow depth of 0.96 m and takes 19.76 hours to reach the final site, Jagat. In contrast, the Scenario 3 (Large) flood wave is far more rapid and destructive, reaching Site 1 in only 0.15 hours and arriving at Jagat in just 4.6 hours. The increase in destructive potential is evident in the hydraulic data. At Site 1 (Samagaon), the maximum flood depth increases dramatically from 0.96 m in Scenario 1 to 12.69 m in Scenario 3, while the maximum velocity skyrockets from a manageable 1.94 m/s to a highly destructive 15.62 m/s. The inundation maps in Figure 12 visually confirms these findings. The most striking feature is the extensive, unconfined flooding at Site 1 (Samagaon) in Scenarios 2 and 3, where the inundation covers a wide portion of the valley floor where the settlement is located. While the flow becomes more channel-bound downstream, the maps clearly show significantly greater depths and widths for the larger scenarios, underscoring the severe risk posed to all downstream sites.

https://doi.org/10.5194/egusphere-2025-4454
Preprint. Discussion started: 29 September 2025

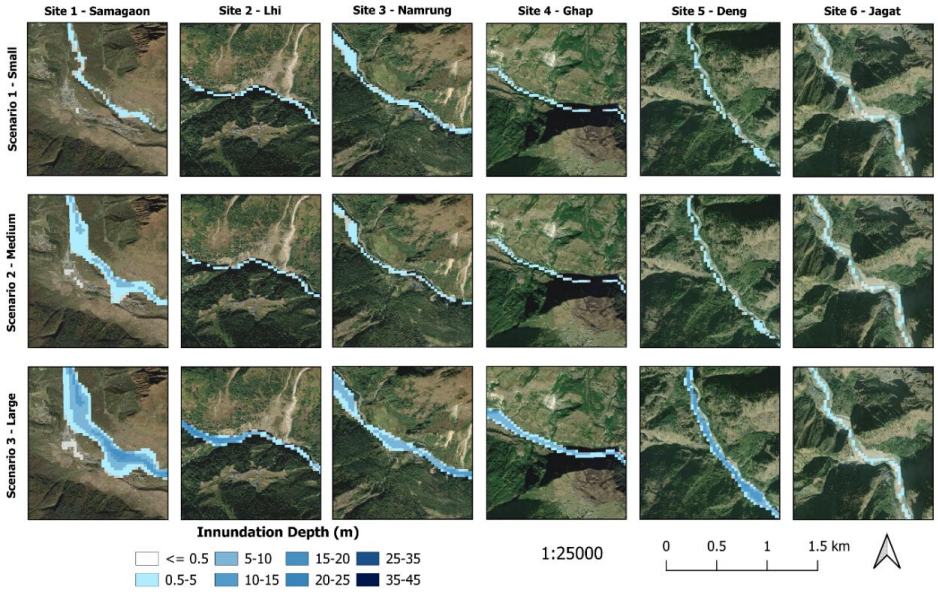

Figure 12 Flood inundation depth maps for three avalanche-triggered scenarios across six downstream monitoring sites, shown using a color scale (© Google Maps 2025).

576 **Table 5** Hydraulic characteristics and flood arrival times for avalanche-triggered GLOF scenarios
577 at downstream monitoring sites

	Flood arrival time (hrs)			Max flood depth (m)			Max flood velocity (m/s)		
Sites	**Sc-1**	**Sc-2**	**Sc-3**	**Sc-1**	**Sc-2**	**Sc-3**	**Sc-1**	**Sc-2**	**Sc-3**
Site 1	0.43	0.15	0.15	0.96	5.82	12.69	1.94	9.49	15.62
Site 2	5.04	1.02	0.5	2.47	2.47	16.09	1.52	1.83	8.24
Site 3	6.76	1.82	0.7	0.56	2.3	11.92	1.86	2.01	6.04
Site 4	9.41	3.32	0.96	0.73	0.83	11.9	1.14	1.38	2.26
Site 5	13.01	6.19	1.45	0.57	0.57	11.13	2.49	2.55	4.97
Site 6	19.76	12.84	4.6	0.86	1.04	1.22	0.93	0.93	1.37

Flow parameters derived from HEC-RAS 2D modeling showing flood arrival times (including initial avalanche travel time to lake), maximum flood depths, and peak velocities for three scenarios (Sc-1, Sc-2, Sc-3) across six sites from Samagaon (Site 1) to Jagat (Site 6).

578

https://doi.org/10.5194/egusphere-2025-4454
Preprint. Discussion started: 29 September 2025

3.8 Comparison with an Alternative Hazard Scenario: Dam Breach vs Lake Overspill

A critical comparison with the concurrent study by Poudel et al. (2025) provides essential context for understanding the spectrum of GLOF hazards at Birendra Lake. The fundamental distinction lies in triggering mechanisms and physical processes: Poudel et al.'s research models a hypothetical moraine dam breach scenario involving structural failure of the terminal moraine, whereas this study simulates avalanche-triggered lake overspill through displacement wave generation, which is a process directly analogous to the observed 21 April 2024 event. Peak discharge comparisons reveal the contrasting hazard magnitudes: dam breach scenarios generate extreme peak flows of 853-10,631 m^3/s through rapid lake drainage, while overspill scenarios produce more moderate but still significant peaks of 133-2,365 m^3/s through displacement-driven outflow. This order-of-magnitude difference reflects the distinct physical processes, where breach scenarios involve catastrophic structural failure, releasing large fractions of total lake volume, versus overspill events, displacing limited water volumes (less than 0.2% of lake capacity) while maintaining moraine integrity.

Temporal characteristics further distinguish these processes: dam breach events typically exhibit sustained high discharge over hours as the breach widens and lake drains, while avalanche-triggered overspill demonstrates impulsive, short-duration pulses consistent with the 8–10 minute significant outflow documented in this study. This temporal distinction has critical implications for warning systems, as overspill events provide even less reaction time than breach scenarios. Process probability assessments suggest that overspill events represent higher-frequency, moderate-impact hazards compared to the' lower-frequency, extreme-impact nature of complete dam failures. The April 2024 event demonstrates the immediate relevance of avalanche-triggered processes, while structural dam failure remains a longer-term concern requiring ongoing moraine stability monitoring. Both studies independently validate that Birendra Lake poses multi-modal GLOF threats requiring comprehensive risk management strategies. The overspill hazard documented here represents the immediate, observable threat that has already materialised, while Poudel et al.'s breach scenarios quantify potential future catastrophic risks under extreme conditions. This dual characterisation provides the hazard spectrum necessary for effective disaster risk reduction planning in the Manaslu region.

https://doi.org/10.5194/egusphere-2025-4454
Preprint. Discussion started: 29 September 2025

3.9 Uncertainty Discussion and Limitations

Uncertainty sources were identified using established guidelines for natural-hazard modelling. The main limitations are:

- Process simplifications – Avalanche-generated impulse waves are not simulated, and dam-erosion or sediment feedback are excluded, so peak discharge and arrival time may be misestimated.
- Terrain data (30 m DEM) – The grid smooths narrow channels and levees that steer flow, leading to location-specific depth and velocity errors.
- Lake geometry & roughness – Bathymetry is inferred from empirical area–volume curves, and Manning's *n* values come from literature; both introduce unknown bias into the hydrograph.
- Scenario assumptions – A single, fixed displacement ratio and three deterministic avalanche sizes replace a full probabilistic ensemble, masking low-likelihood, high-impact events.
- Temporal factors – The modelling does not account for seasonal variations in lake levels or potential dam erosion processes that could modify flood characteristics.

4 CONCLUSION AND RECOMMENDATIONS

4.2 CONCLUSION

This research establishes the first comprehensive quantitative assessment of avalanche-triggered GLOF hazards at Birendra Lake, demonstrating that medium to large-scale ice avalanches ($\geq 5.3 \times 10^5$ m³) originating from the Manaslu Glacier pose a critical and imminent threat with the potential to trigger catastrophic overspill flooding. The integrated RAMMS-HEC-RAS modelling approach successfully simulated the complete hazard cascade from avalanche release to downstream flood propagation, validating the physically viable overspill mechanism observed during the April 21, 2024, event. All three simulated scenarios reached Birendra Lake with substantial mass retention ranging from 62% to 86%, while generating maximum flow velocities up to 72.8 m/s, demonstrating the high-energy nature of these cascading processes consistent with documented Himalayan avalanche behaviour.

https://doi.org/10.5194/egusphere-2025-4454
Preprint. Discussion started: 29 September 2025

The non-linear relationship between avalanche volume and flood severity is a critical finding for hazard assessment applications. At the same time, the small-volume scenario (51,200 m^3) produced only minor downstream impacts; medium and large scenarios (534,000 m^3 and 1,165,000 m^3, respectively) generated disproportionately severe flood waves that pose significant threats to downstream communities. At Samagaon, the progression from small to large scenarios produces a 13-fold increase in maximum flood depths (0.96m to 12.69m) and an 8-fold surge in peak velocities (1.94 m/s to 15.62 m/s), indicating critical threshold behaviour where moderate increases in avalanche magnitude generate catastrophic downstream amplification.

The temporal compression dynamics represent the most critical finding for disaster risk reduction applications. Flood waves reach Samagaon within 9-26 minutes, depending on avalanche magnitude, with the large scenario generating arrival times comparable to the 6-minute lake-emptying observed at Gongbatongsha and the 3-minute avalanche-to-discharge sequence documented at Imja Tsho. This extreme temporal compression eliminates traditional flood warning paradigms. It necessitates fundamental shifts toward pre-positioned emergency response rather than reactive evacuation strategies, aligning with established patterns of impulsive, short-duration GLOF behaviour across comparable Himalayan systems.

Despite methodological simplifications inherent in the displacement efficiency assumptions and topographic resolution constraints, the modelling results demonstrate strong qualitative alignment with observed characteristics from the April 2024 event, including rapid onset, overspill mechanism, and downstream impact patterns. The conservative parameter selection (45% displacement efficiency derived from established Himalayan GLOF modelling practices, literature-based roughness values) suggests that results represent reasonable lower-bound estimates for planning applications while maintaining physical consistency with documented cascading processes.

These findings contribute essential quantitative evidence to the growing understanding of cascading mountain hazards under accelerating climate change, with broader implications for hundreds of similar glacier-lake systems throughout the Himalayas, where steep glacier termini create comparable geometric conditions for avalanche-triggered processes. The study establishes both immediate risk insights for the vulnerable Manaslu region and methodological contributions

https://doi.org/10.5194/egusphere-2025-4454
Preprint. Discussion started: 29 September 2025

to climate adaptation planning, providing a replicable framework for rapid hazard assessment in data-scarce mountain environments and supporting the urgent need for comprehensive disaster risk reduction strategies in one of the world's hazard-prone regions.

4.3 RECOMMENDATIONS

The recommendations of our study include:

a. Immediate implementation of a multi-component early warning system is essential, incorporating glacier stability sensors, lake level monitoring, and automated downstream alerts, given the extremely rapid flood arrival times (minutes to critical settlements).
b. Hazard-based land use planning should implement the detailed flood inundation maps as regulatory tools, prohibiting new construction within high-hazard zones and assessing existing infrastructure vulnerability, particularly in Samagaun's vulnerable valley floor area.
c. Community preparedness programs must be developed with targeted risk communication and evacuation procedures integrated into existing disaster risk reduction frameworks.
d. Future research priorities include conducting detailed bathymetric surveys of Birendra Lake to reduce critical uncertainties, acquiring high-resolution topographic data, developing explicit impulse wave generation models, and integrating geotechnical dam stability analysis.
e. Long-term monitoring frameworks combining remote sensing with in-situ measurements should be established to track system evolution and provide validation data for model refinement.
f. Extending the integrated modelling approach to other high-risk glacial lake systems throughout the Himalayas to support regional climate change adaptation planning and develop standardised protocols for rapid hazard assessment in data-scarce environments.

CODE AVAILABILITY

Not applicable

DATA AVAILABILITY

Contact the corresponding author for more information on access to datasets.

https://doi.org/10.5194/egusphere-2025-4454
Preprint. Discussion started: 29 September 2025

AUTHOR CONTRIBUTIONS

Mohan, Ragini, Rijan and Sujan designed the study. Ragini and Sujan contributed to data collection. Ragini and Sujan performed the data analysis and interpretation. Mohan, Ragini, Rijan, and Sujan prepared the manuscript with contributions from all co-authors. Mohan and Rijan supervised the research.

COMPETING INTERESTS

The contact author has declared that none of the authors has any competing interests.

ACKNOWLEDGEMENTS

We thank the National Trust for Nature Conservation (NTNC)-Manaslu Conservation Area Project (MCAP) for their generous financial support. The grant provided by NTNC-MCAP played a crucial role in completing this project. In addition, we would like to express our sincere gratitude to the RAMMS development team at the WSL Institute for Snow and Avalanche Research SLF for kindly providing the RAMMS software license.

FINANCIAL SUPPORT

This research has been supported by the National Trust for Nature Conservation- Manaslu Conservation Area Project (NTNC-MCAP).

REFERENCES

Acharya, A., Steiner, J. F., Walizada, K. M., Zakir, Z. H., Ali, S., Caiserman, A., and Watanabe, T.: Snow and ice avalanches in High Mountain Asia – scientific, local and indigenous knowledge, Nat. Hazards Earth Syst. Sci. Discuss., 2023, 1–35, https://doi.org/10.5194/nhess-23-2569-2023, 2023

Alean, J.: Ice avalanches: some empirical information about their formation and reach, J. Glaciol., 31, 324–333, doi:10.3189/S0022143000006663, 1985.

Aristizábal, E., Duque, C., Botero, B., and Arévalo, D.: Probabilistic cascade modeling for enhanced flood and landslide hazard assessment: integrating multi-model approaches in the La Liboriana River basin, Water, 16, 2404, https://doi.org/10.3390/w16172404, 2024.

https://doi.org/10.5194/egusphere-2025-4454
Preprint. Discussion started: 29 September 2025

Bartelt, P., Buser, O., and Platzer, K.: Snow avalanche simulation using the Voellmy–Salm rheology: critical parameterization issues, Cold Reg. Sci. Technol., 69, 72–81, https://doi.org/10.1016/j.coldregions.2011.12.004, 2012.

Brunner, G. W.: HEC-RAS River Analysis System User's Manual, U.S. Army Corps of Engineers, Hydrologic Engineering Center, https://www.hec.usace.army.mil/confluence/hec-rasmanuals:hec-ras-2d-users-manual (last access: 24 September 2025), 2016.

Bühler, Y., von Rickenbach, D., Stoffel, A., Margreth, S., Stoffel, L., and Christen, M.: Automated identification of potential snow avalanche release areas based on digital elevation models, Nat. Hazards Earth Syst. Sci., 13, 1321–1335, https://doi.org/10.5194/nhess-13-1321-2013, 2013

Byers, A. C., Chand, M. B., Lala, J., Shrestha, M., Byers, E. A., and Watanabe, T.: Reconstructing the history of glacial lake outburst floods (GLOF) in the Kanchenjunga Conservation Area, East Nepal: an interdisciplinary approach, Sustainability, 12, 5407, https://doi.org/10.3390/su12135407, 2020.

Byers, A. C., Rounce, D. R., Shugar, D. H., et al.: A rockfall-induced glacial lake outburst flood, Upper Barun Valley, Nepal, Landslides, 16, 533–549, https://doi.org/10.1007/s10346-018-1079-9, 2019.

Carrivick, J. L. and Tweed, F. S.: A global assessment of the societal impacts of glacier outburst floods, Glob. Planet. Change, 144, 1–16, https://doi.org/10.1016/j.gloplacha.2016.07.001, 2016.

Casteller, A., Christen, M., Villalba, R., Martínez, H., Stöckli, V., Leiva, J. C., and Bartelt, P.: Validating numerical simulations of snow avalanches using dendrochronology: the Cerro Torre event in Argentina, Nat. Hazards Earth Syst. Sci., 8, 433–443, https://doi.org/10.5194/nhess-8-433-2008, 2008.

Chand, M. B. and Watanabe, T.: Development of supraglacial ponds in the Everest region, Nepal, between 1989 and 2018, Remote Sens., 11, 1058, https://doi.org/10.3390/rs11091058, 2019.

Chaulagain, M., Chand, M. B., Pradhananga, D., Dhungana, B., Kayastha, R. B., and Manandhar, S.: Recurring avalanche hazards at Birendra Lake, Manaslu region: interdisciplinary insights from the 21 April 2024 avalanche event, J. Tourism Himalayan Adventures, 7, 59–77, https://doi.org/10.3126/jtha.v7i1.80884, 2025.

Chisolm, R. E. and McKinney, D. C.: Dynamics of avalanche-generated impulse waves: three-dimensional hydrodynamic simulations and sensitivity analysis, Nat. Hazards Earth Syst. Sci., 18, 1373–1393, https://doi.org/10.5194/nhess-18-1373-2018, 2018.

https://doi.org/10.5194/egusphere-2025-4454
Preprint. Discussion started: 29 September 2025

Chow, V. T.: Open-Channel Hydraulics, McGraw-Hill, New York, USA, 680 pp., 1959. ISBN: 9781260469707

Christen, M., Kowalski, J., and Bartelt, P.: RAMMS: numerical simulation of dense snow avalanches in three-dimensional terrain, Cold Reg. Sci. Technol., 63, 1–14, https://doi.org/10.1016/j.coldregions.2010.04.005, 2010.

Clague, J. J. and Evans, S. G.: A review of catastrophic drainage of moraine-dammed lakes in British Columbia, Quat. Sci. Rev., 19, 1763–1783, https://doi.org/10.1016/S0277-3791(00)00090-1, 2000.

Copernicus Emergency Management Service: Analysing risks of dam breaks and spillage, https://mapping.emergency.copernicus.eu/about/risk-and-recovery-mapping-portfolio/analysing-risks-of-dam-breaks-and-spillage/ (last access: 24 September 2025), 2025.

Costa, J. E. and Schuster, R. L.: The formation and failure of natural dams, Geol. Soc. Am. Bull., 100, 1054–1068, https://doi.org/10.1130/0016-7606(1988)100<1054:TFAFON>2.3.CO;2, 1988.

Emmer, A. and Cochachin, A.: The causes and mechanisms of moraine dam failure: a detailed analysis of the Lake Palcacocha disaster (Cordillera Blanca, Peru, 1941), Nat. Hazards, 65, 1739–1758, https://doi.org/10.1007/s11069-012-0433-9, 2013.

Feldman, A. D.: Hydrologic Modeling System HEC-HMS Technical Reference Manual, U.S. Army Corps of Engineers, Hydrologic Engineering Center, https://www.hec.usace.army.mil/confluence/hmsdocs:hec-hms-technical-reference-manual (last access: 24 September 2025), 2000.

Gabl, R., Seibl, J., Gems, B., and Aufleger, M.: Dynamics of avalanche-generated impulse waves: three-dimensional hydrodynamic simulations and sensitivity analysis, Nat. Hazards, 87, 1191–1208, https://doi.org/10.1007/s11069-017-2811-7, 2017.

Gauer, P., Issler, D., Lied, K., Kristensen, K., and Sandersen, F.: Snow avalanche mass and impact pressure dynamics derived from high-speed measurements, Cold Reg. Sci. Technol., 51, 118–133, https://doi.org/10.1016/j.coldregions.2007.05.019, 2008.

Heller, V., Hager, W. H., and Minor, H. E.: Composite modelling of subaerial landslide–tsunamis in different water-body geometries and novel insight into slide and wave kinematics, Coast. Eng., 56, 668–681, https://doi.org/10.1016/j.coastaleng.2015.12.004, 2016.

Hock, R., Rasul, G., Adler, C., Cáceres, B., Gruber, S., Hirabayashi, Y., Jackson, M., Kääb, A., Kang, S., Kutuzov, S., Milner, A., Molau, U., Morin, S., Orlove, B., and Steltzer, H.: High Mountain Areas, in: IPCC Special Report on the Ocean and Cryosphere in a Changing Climate,

https://doi.org/10.5194/egusphere-2025-4454
Preprint. Discussion started: 29 September 2025

edited by: Pörtner, H.-O., Roberts, D. C., Masson-Delmotte, V., Zhai, P., Tignor, M., Poloczanska, E., Mintenbeck, K., Alegría, A., Nicolai, M., Okem, A., Petzold, J., Rama, B., and Weyer, N. M., Cambridge University Press, Cambridge, UK and New York, NY, USA, 131–202, https://doi.org/10.1017/9781009157964.004, 2019.

Huggel, C., Kääb, A., Haeberli, W., Teysseire, P., and Paul, F.: Remote sensing-based assessment of hazards from glacier-lake outbursts: a case study in the Swiss Alps, Can. Geotech. J., 39, 316–330, https://doi.org/10.1139/t01-093, 2002a.

Huggel, C., Kääb, A., Salzmann, N., Teysseire, P., and Paul, F.: Loss of ice from lakes on Kilimanjaro and its implications for hydrology, Glob. Planet. Change, 35, 81–99, https://doi.org/10.1016/S0921-8181(02)00108-8, 2002b.

Huss, M., Bookhagen, B., Huggel, C., Jacobsen, D., Bradley, R. S., Clague, J. J., et al.: Toward mountains without permanent snow and ice, Earth's Future, 5, 418–435, https://doi.org/10.1002/2016EF000514, 2017.

Khadka, N., Ghimire, S. K., Sharma, S., and Hamal, K.: Rapidly expanding glacial lakes in Nepal Himalaya, Jalawaayu, 2, 45–55, https://doi.org/10.3126/jalawaayu.v2i1.45393, 2022.

Khadka, N., Zheng, G., Chen, X., Zhong, Y., Allen, S. K., and Gouli, M. R.: An ice-snow avalanche triggered small glacial lake outburst flood in Birendra Lake, Nepal Himalaya, Nat. Hazards, 121, 6357–6365, https://doi.org/10.1007/s11069-024-07014-0, 2025.

Klimeš, J., Benešová, M., Vilímek, V., Bouška, P., and Rapre, A. C.: The reconstruction of a glacial lake outburst flood using HEC-RAS and its significance for future hazard assessments: an example from Lake 513 in the Cordillera Blanca, Peru, Nat. Hazards, 71, 1617–1638, https://doi.org/10.1007/s11069-013-0968-4, 2014.

Lala, J. M., Rounce, D. R., and McKinney, D. C.: Modeling the glacial lake outburst flood process chain in the Nepal Himalaya: reassessing Imja Tsho's hazard, Hydrol. Earth Syst. Sci., 22, 3721–3737, https://doi.org/10.5194/hess-22-3721-2018, 2018.

Lee, Y. S., Shin, S., Baek, S., Kim, H. K., and Kim, M. J.: GIS-based flood assessment using hydraulic modeling and open data: a case study of the Nakdong River, Appl. Sci., 15, 2520, https://doi.org/10.3390/app15052520, 2023.

Maharjan, S. B., Dangol, P., Shrestha, F., Bajracharya, B., and Sherpa, T. C.: Insights behind the unexpected flooding in the Budhi Gandaki River, Gorkha, Nepal, International Centre for Integrated Mountain Development (ICIMOD), https://www.icimod.org/cryosphere-

https://doi.org/10.5194/egusphere-2025-4454
Preprint. Discussion started: 29 September 2025

water/insights-behind-the-unexpected-flooding-in-the-budhi-gandaki-river-gorkha-nepal/ (last access: 24 September 2025), 2024.

Mandal, A., Adhikari, A., Shakya, A., Dwivedi, A., Bhusal, A., Shrestha, A., and Kafle, M. R.: Hydrodynamic modelling of glacial lake outburst flood in Lower Barun Lake, Discover Civil Engineering, 2, 18, https://doi.org/10.1007/s44290-025-00176-1, 2025.

Maskey, S., Kayastha, R. B., and Kayastha, R.: Glacial lake outburst floods (GLOFs) modelling of Thulagi and Lower Barun glacial lakes of Nepalese Himalaya, Prog. Disaster Sci., 7, 100106, https://doi.org/10.1016/j.pdisas.2020.100106, 2020.

Mehar, P.: Avalanche sets off glacial lake outburst in Nepal: why GLOFs recur in Himalayas and how to prevent them, ThePrint, https://theprint.in/science/avalanche-sets-off-glacial-lake-outburst-in-nepal-why-glofs-recur-in-himalayas-how-to-prevent-them/2051617/ (last access: 24 September 2025), 2024.

Mergili, M., Pudasaini, S. P., Emmer, A., Fischer, J. T., Cochachin, A., and Frey, H.: Computational experiments on the 1962 and 1970 landslide events at Huascarán (Peru) with r.avaflow, Nat. Hazards Earth Syst. Sci., 20, 1233–1259, https://doi.org/10.1016/j.geomorph.2018.08.032, 2020.

Mergili, M., Pudasaini, S. P., and Krautblatter, M.: New thermomechanical model for rock/ice avalanches, Swiss Federal Institute for Forest, Snow and Landscape Research (WSL), https://www.wsl.ch/en/news/new-thermomechanical-model-for-rock/ice-avalanches/ (last access: 24 September 2025), 2022.

Østrem, G. and Brugman, M.: Glacier Mass-Balance Measurements: A Manual for Field and Office Work, NHRI, Report No. 4, 224 pp., 1991. ISBN 0-662-19000-9

Poudel, U., Gouli, M. R., Hu, K., Khadka, N., Regmi, R. K., and Thapa, B. R.: Multi-breach GLOF hazard and exposure analysis of Birendra Lake in the Manaslu Region of Nepal, Nat. Hazards Res., [vol./pages needed], https://doi.org/10.1016/j.nhres.2025.03.007, 2025.

Richards, K. S. and Reddy, K. R.: Critical appraisal of piping phenomena in earth dams, Bull. Eng. Geol. Environ., 66, 381–402, https://doi.org/10.1007/s10064-007-0098-0, 2007.

Rounce, D. R., Quincey, D. J., and McKinney, D. C.: Debris-covered glacier energy balance model for Imja–Lhotse Shar Glacier in the Everest region of Nepal, The Cryosphere, 9, 2295–2310, https://doi.org/10.5194/tc-9-2295-2015, 2015.

https://doi.org/10.5194/egusphere-2025-4454
Preprint. Discussion started: 29 September 2025

Sattar, A., Haritashya, U. K., Kargel, J. S., Leonard, G. J., Shugar, D. H., and Chase, D. V.: Modeling lake outburst and downstream hazard assessment of the Lower Barun Glacial Lake, Nepal Himalaya, J. Hydrol., 598, 126208, 2021.

Sattar, A., Haritashya, U. K., Kargel, J. S., and Karki, A.: Transition of a small Himalayan glacier lake outburst flood to a giant trans-border flood and debris flow, Sci. Rep., 12, 12421, 2022.

Schneider, D., Huggel, C., Cochachin, A., Guillén, S., and García, J.: Mapping hazards from glacier lake outburst floods based on modelling of process cascades at Lake 513, Carhuaz, Peru, Adv. Geosci., 35, 145–155, 2014. https://doi.org/10.5194/adgeo-35-145-2014, 2014.

SLF: RAMMS::Extended – RAMMS – Rapid mass movement simulation, https://ramms.ch/rammsextended/ (last access: 24 September 2025), 2025.

Somos-Valenzuela, M. A., Chisolm, R. E., Rivas, D. S., Portocarrero, C., and McKinney, D. C.: Modeling a glacial lake outburst flood process chain: the case of Lake Palcacocha and Huaraz, Peru, Hydrol. Earth Syst. Sci., 22, 3721–3737, https://doi.org/10.5194/hess-22-3721-2018, 2018.

Vera Valero, C., Wever, N., Bühler, Y., Stoffel, L., Margreth, S., and Bartelt, P.: Modelling wet-snow avalanche runout to assess road safety at a high-altitude mine in the central Andes, Nat. Hazards Earth Syst. Sci., 15, 731–749, https://doi.org/10.5194/nhess-15-731-2015, 2015.

Walder, J. S., Watts, P., Sorensen, O. E., and Janssen, K.: Tsunamis generated by subaerial mass flows, J. Geophys. Res.-Solid Earth, 108, B5, https://doi.org/10.1029/2002JB002102, 2003.

Wang, X., Guo, X., Yang, C., Liu, Q., Wei, J., Zhang, Y., et al.: Glacial lake inventory of High-Mountain Asia in 1990 and 2018 derived from Landsat images, Earth Syst. Sci. Data, 12, 2169–2182, https://doi.org/10.5194/essd-12-2169-2020, 2020.

Westoby, M. J., Glasser, N. F., Brasington, J., Hambrey, M. J., Quincey, D. J., and Reynolds, J. M.: Modelling outburst floods from moraine-dammed glacial lakes, Earth Surf. Process. Landf., 39, 665–674, https://doi.org/10.1016/j.earscirev.2014.03.009, 2014.

Worni, R., Huggel, C., Clague, J. J., Schaub, Y., and Stoffel, M.: Coupling glacial lake impact, dam breach, and flood processes: a modeling perspective, Geomorphology, 224, 161–176, https://doi.org/10.1016/j.geomorph.2014.06.031, 2015.

Worni, R., Huggel, C., and Stoffel, M.: Glacial lakes in the Indian Himalayas – from an area-wide glacial-lake inventory to on-site and modeling-based risk assessment of critical glacial lakes, Sci. Total Environ., 468–469, 71–84, https://doi.org/10.1016/j.scitotenv.2013.08.038, 2014.

https://doi.org/10.5194/egusphere-2025-4454
Preprint. Discussion started: 29 September 2025

878 Yang, F., Duan, K., Zhong, X., and Huang, X.: Refining lake volume estimation and critical depth
879 identification for GLOF modeling, The Cryosphere, 18, 5921–5935, https://doi.org/10.5194/tc-18-
880 5921-2024, 2024.
881 Yao, X., Liu, S., Sun, M., Wei, J., and Guo, W.: Volume calculation and analysis of the changes
882 in moraine-dammed lakes in the North Himalaya: a case study of Longbasaba Lake, J. Glaciol.,
883 58, 753–760, https://doi.org/10.3189/2012JoG11J180, 2012.
884 Zitti, G., Ancey, C., Postacchini, M., and Brocchini, M.: Impulse waves generated by snow
885 avalanches: momentum and energy transfer to a water body, J. Geophys. Res.-Earth Surf., 121,
886 2399–2423, https://doi.org/10.1002/2016JF003956, 2016.
887

888 **APPENDICES**

889 **Appendix A**

890 Small simulation showing maximum height, velocity, and pressure

891
892
893
894
895
896
897
898
899
900
901
902

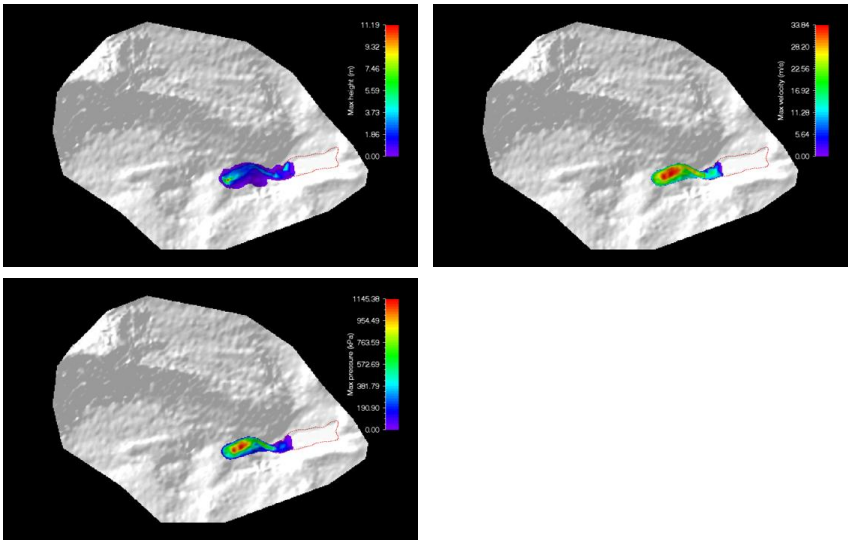

903
904
905
906

https://doi.org/10.5194/egusphere-2025-4454
Preprint. Discussion started: 29 September 2025

Appendix B

Medium simulation showing maximum height, velocity, and pressure

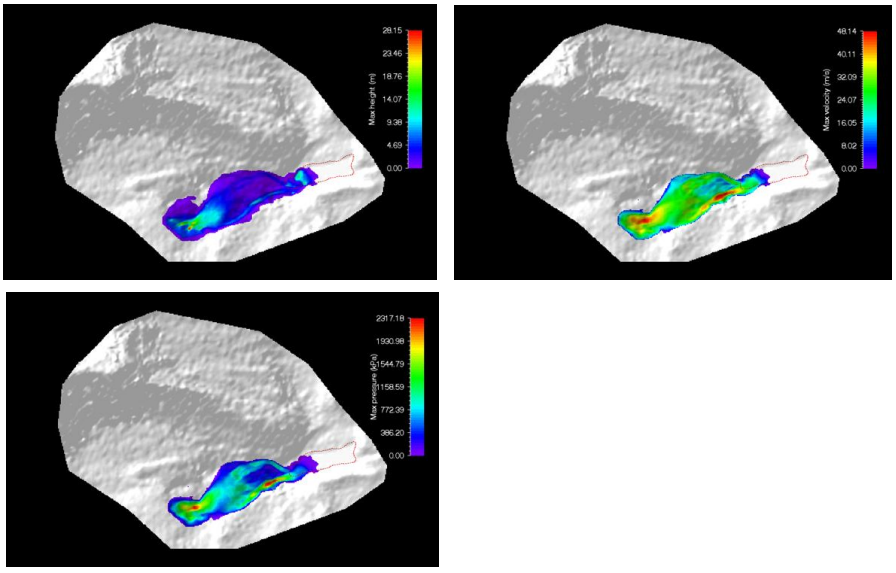

Appendix C

Large Simulation showing maximum height, velocity, and pressure

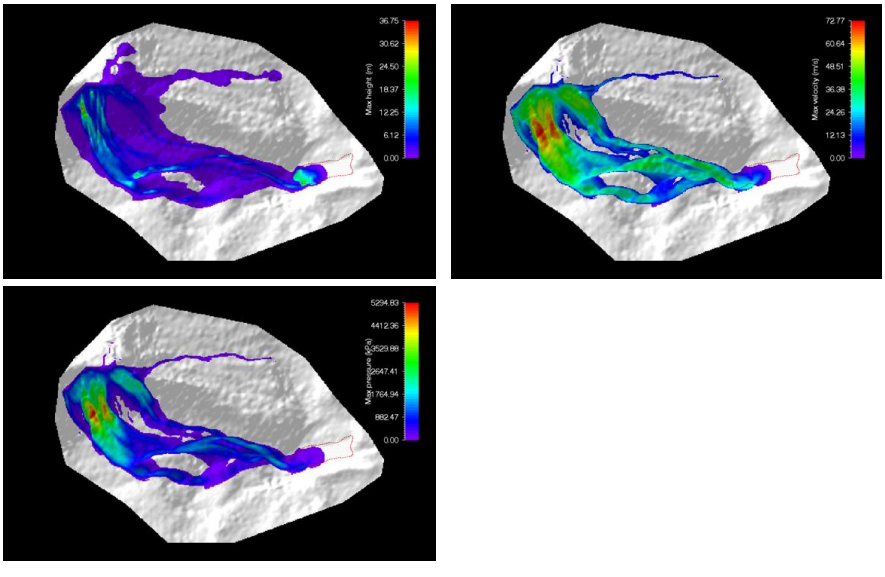

https://doi.org/10.5194/egusphere-2025-4454
Preprint. Discussion started: 29 September 2025

Appendix D

Avalanche Flow Simulation